Velocity of Sound and Viscosity for Pure HFC Refrigerants and their Mixtures in High Pressure Gas Region[1]

Jurij Avsec[2,3]

[2]University of Maribor, Faculty of Mechanical Engineering, Smetanova 17, 2000 Maribor, P.O. BOX 224, SLOVENIA.

[3]To whom corresspondence should be addresseed. Email: jurij.avsec@uni-mb.si

Abstract:

The paper features a theoretical model for computing the speed of sound and the viscosity in the real gas phase of pure refrigerants and their mixtures. To calculate the viscosity of real fluids models on basis of the Lennard-Jones intermolecular potential with simultaneous consideration of the influence of multipole moments have been applied.

Keywords: Speed of sound, viscosity, refrigerants, real gas, mixtures

1. INTRODUCTION

In technical practice fluid mechanics processes are of vital importance. The mathematical theory of chaos may in the future contribute to our understandings of turbulent flow. At this time in practical engineering for the prediction of turbulence is almost in all cases used the classical models such as k-ε or k-ω model. Today are on the market many excellent models (CFX, FIRE, IDEAS,….) for the use in fluid engineering. One of the main problems of presented models is hidden in relatively weak database of thermophysical properties. Almost in all cases are thermophysical properties represented as constants independent on the temperature and pressure field. In this paper we try to present the importance of thermophysical properies for the studying of advanced fluid mechanics.

In order to design devices of this field of activity, it is necessary to be familiar with the equilibrium and nonequilibrium thermodynamic properties of state in a one and two phase environment for pure compounds and their mixtures.

In these paper we developed the mathematical model of computing the transport properties of state.

2. VELOCITY OF SOUND

In this paper our interest is focused on the calculation of speed of sound. The speed of sound refers to the speed of the mechanical longitudinal pressure waves propagating through a medium. It is a very important parameter in the study of compressible fluid flows and in some applications (acoustic resonance level gauge).

The propagation of sonic waves for real fluids is almost in all cases nearly isentropic. Therefore, we can calculate the isentropic speed of sound for a real fluid c_0:

$$c_0 = \sqrt{-V^2\left(\frac{\partial P}{\partial V}\right)_{S,\psi}\frac{1}{M}}, \qquad (1)$$

where M is the molecular mass, S is the entropy and ψ is the molar concentration.

3. INTERMOLECULAR FORCES

Molecules are composed of positive and negative charges. According to Coulomb's law of electrostatics the charges interact and the interaction energy between the molecules in the system is called intermolecular energy. Hence, we say that intermolecular forces are of electrostatic nature.

The analytical computation of intermolecular potential is extremely complex [1-4]. As far as certain simple systems are concerned the problem is soluble, although the equations thus obtained are very complicated. This is why further analytical solutions of a configuration integral is exceptionally difficult. In general, the assumption for the sum of repulsive (rep) and attractive (att) force is sufficiently accurate. If the intermolecular potential is denoted by u then the equation below can be written as:

$$u = u_{rep} + u_{att} \qquad (2)$$

The occurrence of the **repulsive force** is associated with the Pauli exclusion principle. If two molecules approach one another within a very short distance, so that the electronic clouds of both mlecules begin to coincide, certain electrons in the molecule have to move to higher energy levels due to the exclusion principle, made possible only through the supply of sufficient energies, resulting in the occurrence of the repulsive force.

4. IMPACT OF ANISOTROPIC POTENTIALS ON THERMODYNAMIC FUNCTIONS OF STATE

There are several methods to compute the influence of anisotropic potentials [9-27]. In the present paper those models were used which yielded favorable results in practical computations for a large number of components and within a relatively wide range of densities and temperatures.

Using the perturbation expansion around the reference potential one can then write the configuration effect to the free energy as:

$$\frac{A_{conf}}{Nk_BT} = \frac{A^{LJ}}{Nk_BT} + \frac{A^{\lambda}}{Nk_BT} + \frac{A^{\lambda\lambda}}{Nk_BT} + \frac{A^{\lambda\lambda\lambda}}{Nk_BT} \tag{3}$$

The free energy of Lennard-Jones's fluid A^{LJ} was calculated using the Johnson-Zolweg-Gubbins's (JZG) model [5].

We consider rigid nonlinear molecules [1] with enough symmetry so that the principal axes of the quadrupole tensor coincide. The multipole expansion is terminated at the quadrupole term. Intermolecular repulsion interaction is modeled by the Lennard-Jones r^{-12} law. The induction interactions are formulated in the isotropic polarizibility approximation. Intermolecular interactions are limited to the second-order term, and cross terms between intermolecular interactions are not considered.

First order terms:

Inductive forces:

$$\left(\frac{A^{\lambda}}{NkT}\right)^{ind} = -4\pi\frac{N}{V}\left(\frac{1}{kT}\right)\alpha\left[\left(\mu_x{}^2 + \mu_y{}^2 + \mu_z{}^2\right)\frac{J(6)}{\sigma^3} + \left(\theta_x{}^2 + \theta_y{}^2 + \theta_z{}^2\right)\frac{J(8)}{\sigma^5}\right]. \tag{4}$$

Second order terms:

Multipole forces:

$$\left(\frac{A^{\lambda\lambda}}{NkT}\right)^{mult-mult} = -\frac{\pi N}{(kT^2)V}\left[\begin{array}{l}\frac{2}{3}\left(\mu_x{}^2+\mu_y{}^2+\mu_z{}^2\right)^2\frac{J(6)}{\sigma^3}\\ +\frac{4}{3}\left(\mu_x{}^2+\mu_y{}^2+\mu_z{}^2\right)\left(\theta_x{}^2+\theta_y{}^2+\theta_z{}^2\right)\frac{J(8)}{\sigma^5}\\ +\frac{56}{45}\left(\mu_x{}^2+\mu_y{}^2+\mu_z{}^2\right)\left(\theta_x{}^2+\theta_y{}^2+\theta_z{}^2\right)\frac{J(10)}{\sigma^7}\end{array}\right] .(5)$$

Inductive forces:

$$\left(\frac{A^{\lambda\lambda}}{NkT}\right)^{ind-ind} = \left(\frac{A^{\lambda\lambda}}{NkT}\right)_A^{ind-ind} + \left(\frac{A^{\lambda\lambda}}{NkT}\right)_B^{ind-ind} .$$

$$\left(\frac{A^{\lambda\lambda}}{NkT}\right)_A^{ind-ind} = -\frac{9N\pi}{V(kT)^2}\alpha^2\left[\begin{array}{l}\frac{2}{45}\left(\mu_x{}^2+\mu_y{}^2+\mu_z{}^2\right)^2\frac{J(12)}{\sigma^9}\\ +\frac{24}{25}\left(\mu_x{}^2\theta_x{}^2+\mu_y{}^2\theta_y{}^2+\mu_z{}^2\theta_z{}^2\right)\frac{J(14)}{\sigma^{11}}\\ +\frac{32}{315}\left(\mu_x{}^2+\mu_y{}^2+\mu_z{}^2\right)\left(\theta_x{}^2+\theta_y{}^2+\theta_z{}^2\right)\frac{J(14)}{\sigma^{11}}\\ +\frac{1024}{4725}\left(\begin{array}{l}\mu_x{}^2\theta_x{}^2+\mu_y{}^2\theta_y{}^2+\mu_z{}^2\theta_z{}^2\\ -\frac{5}{8}\mu_x{}^2\theta_z\theta_y-\frac{5}{8}\mu_y{}^2\theta_x\theta_z-\frac{5}{8}\mu_z{}^2\theta_x\theta_y\end{array}\right)\frac{J(14)}{\sigma^{11}}\\ +\frac{24}{315}\left(\theta_x{}^2+\theta_y{}^2+\theta_z{}^2\right)^2\frac{J(16)}{\sigma^{13}}\end{array}\right] .(6)$$

$$\left(\frac{A^{\lambda\lambda}}{Nk_BT}\right)_B^{ind-ind} =$$

$$-\frac{9\pi^2N^2}{(VkT)^2}\sigma^2\alpha^2\left[\begin{array}{l}\frac{48}{25}\left(\mu_x{}^2\theta_x{}^2+\mu_y{}^2\theta_y{}^2+\mu_z{}^2\theta_z{}^2\right)\frac{L(1,7,7)}{\sigma^{10}}+\\ \frac{4}{45}\left(\mu_x{}^2+\mu_y{}^2+\mu_z{}^2\right)\frac{L(2,6,6)}{\sigma^8}+\\ \frac{64}{315}\left(\mu_x{}^2+\mu_y{}^2+\mu_z{}^2\right)\left(\theta_x{}^2+\theta_y{}^2+\theta_z{}^2\right)\frac{L(2,6,8)}{\sigma^{10}}+\\ \frac{256}{2205}\left(\theta_x{}^2+\theta_y{}^2+\theta_z{}^2\right)\frac{L(2,8,8)}{\sigma^{12}}+\\ \frac{2048}{4725}\left(\begin{array}{l}\mu_x{}^2\theta_x{}^2+\mu_y{}^2\theta_y{}^2+\mu_z{}^2\theta_z{}^2-\frac{5}{8}\mu_x{}^2\theta_z\theta_y\\ -\frac{5}{8}\mu_y{}^2\theta_x\theta_z-\frac{5}{8}\mu_z{}^2\theta_x\theta_y\end{array}\right)\frac{L(3,7,7)}{\sigma^{10}}\\ +\frac{16}{441}\left(\theta_x{}^2+\theta_y{}^2+\theta_z{}^2\right)^2\frac{L(4,8,8)}{\sigma^{12}}\end{array}\right] \quad (7)$$

The structural properties of the Lennard-Jones potential are introduced via the *J* and *L* integrals expressed as:

$$\begin{aligned}J(n) &= \int_0^\infty \frac{1}{r^{*n}} g_{LJ} r^{*2}\cdot dr^*,\\ L(l;n,n') &= \int_0^\infty\int_0^\infty\int_{-1}^{1} P_l(\cos\phi_1) g_{LJ3} r_{12}^{*(2-n)} r_{13}^{*(2-n')} dr_{12}^* dr_{13}^* d(\cos\phi_1),\\ r^* &= \frac{r}{\sigma},\end{aligned} \quad (8)$$

where g_{LJ} and g_{LJ3} are pair and triplet radial distributions function[3] for the LJ potential, $P_l(\cos\phi_l)$ is the Legendre function and ϕ_l is the internal angle at molecule 1 for the triangle formed by molecules 1,2 and 3.

The *J* and *L* integrals are calculated by numerical integration over tabulated pair correlation functions. We calculated the *J* and *L* integrals with the help of simple interpolation equations:Nicolas-Gubbins-Street-Tildesley [1] (LG).

5. MIXTURES

The thermodynamic properties of real mixtures are obtained using the one-fluid theory [1-4]. The molecules interacting with Lennard-Jones potential have parameters σ and ε given by:

$$\sigma^3 = \sum_{i,j} \psi_i \psi_j \sigma_{ij}^{\ 3}, \varepsilon\sigma^3 = \sum_{i,j} \psi_i \psi_j \varepsilon_{ij} \sigma_{ij}^{\ 3}. \tag{9}$$

$$\sigma_{ij} = \frac{\sigma_{ii} + \sigma_{jj}}{2}, \varepsilon_{ij} = \sqrt{\varepsilon_{ii}\varepsilon_{jj}}\ . \tag{10}$$

We calculated all other important parameters with the help of the following mixing rule. For some general parameter *K* we can write:

$$K = \sum_i \psi_i K_i \tag{11}$$

6. KINETIC THEORY OF DILUTE POLYATOMIC GASES

The kinetic theory of dilute gases assumes a macroscopic system at densities low enough so that molecules most of the time move freely and interact through binary encounters only. Neverthless, the densities are high enough to ensure that the effects of molecule-wall collisions can be neglected compared to those from molecule-moleculeencounters. It is woth nothing in this paper the terms “dilute” or “low-density gas” represent a real physical situation, whereas the frequently us expression “zero-density limit” is related to results of a mathematical extrapolation of a density series of a particular transport property at constant temperature to zero density. This paper is predominantly concerned with the transport properties of fluids of practical significance. This means that attention is concentrated upon systems containing polyatomic molecules and upon the traditional transport properties such as the viscosity

and thermal conductivity. The ease of the practical evaluation of the transport properties of a dilute gas by means of these relationships decreases as the complexity of the molecules increases. Thus for a pure monoatomic gas, with no internal degrees of freedom, the calculations are now trivial, consuming minutes on a personal computer. For systems involving atoms and rigid rotors the computations are now almost routine and take hours on work stations. For systems that involve molecules other than rigid rotors the theory is still approximate and calculations are heuristic.

The background transport properties for pure gases are represented as sums of terms for the temperature-dependent dilute-gas contributions and terms for the temperature- and density-dependent residual contributions. Contribution for the critical enhancement are not included in these background functions.

From the Boltzmann equation we can for mono-atomic dilute gases calculate transport properties not far from the Maxwellian [6]. Thease means, that we treat transport phenomena with small temperature or velocity gradients of the molecules. On thease base we can express viscosity and thermal conductivity for single-component gas:

$$\eta_0 = \frac{5kT}{8\Omega^{(2,2)}}\left(1+\frac{3}{49}\left(\frac{\Omega^{(2,3)}}{\Omega^{(2,2)}}-\frac{7}{2}\right)^2\right) \tag{12}$$

where M is molecular mass of the molecule, and $\Omega^{(l,s)}$ is the transport collision integral. For Leenard-Jones intermolecular potential is almost impossibly obtain collsision integrals analytically. Because of difficulty of calculating these integrals, their values are usually taken from published tables. To make computerized calculations more convenient and to improve on the accuracy obtainable by linear interpolation of the

tables we used Neufeld [7] et al. empirical formulation, obtained on the base of numerical simulations and interpolation procedure.

$$\Omega^{(l,s)} = \frac{A}{T^{*B}} + \frac{C}{\exp(DT^*)} + \frac{E}{\exp(FT^*)} + \frac{G}{\exp(HT^*)} + RT^{*B}\sin(ST^{*W} - P) \qquad (13)$$

This Equation contains 12 adjustable parameters and is developed for 16 collision integrals.

For the calculation of transport properties for polyatomic molecules in principle, a quantum mechanical tratment of processes is necessary to account for the changes of internal state. The fully quantum mechanical kinetic theory of polyatomic gases is based on Waldman-Snider [6,8] equation and summarized by McCourt and coworkers. Wang-Chang and Uhlenbeck and independently by de Boer (WCUB) formulated a semiclassical kinetic theory. The quantum mechanical theory has the advantage that it can treat the degeneracy of rotational energy states and is therefore able to describe the effect of magnetic and electric fields on the transport properties. The disadvantage of this theory for practical applications is that it is only formally established for gases with rotational degrees of freedom. On the other hand, the semiclassical theory has the advantages that it treats all forms of internal energy and is the semiclassical limit of the quantum mechanical approach. In the presented paper we used simple expressions for taking into account rotational contributions. Internal modes have, at relatively low temperatures, almost no influence on viscosity and relatively high influence on thermal conductivity.

The dilute gas viscosity is obtained from kinetic theory assuming that a Lennard-Jones (LJ) potential applies and using the expression:

$$\eta_0(T) = 26.69579 \cdot 10^{-1} \frac{\sqrt{MT}}{\Omega^{(2,2)*}\sigma^2}, \tag{14}$$

where η is in Pa s, M is the molecular mass in gmol^{-1}, T is in K, $\Omega^{(2,2)}$ is a collision integral and σ is the Lennard-Jones parameter.

1. Holland-Hanley model (HH) [9,10]. The viscosity of dense Lennard-Jones fluid is found using [9]

$$\eta(\rho, T) = \eta_0(T) + \eta_{ex}(\rho, T) \tag{15}$$

where η_{ex} is excess viscosity due to high density contribution.

$$\eta_{ex} = 10^{-7} \exp\left(a_1 + \frac{a_2}{T}\right) x \left(\exp\left[\left(a_3 + \frac{a_4}{T^{1.5}}\right)\rho^{0.1} + \left(\frac{\rho}{\rho_c} - 1\right)\rho^{1/2}\left(a_5 + \frac{a_6}{T} + \frac{a_7}{T^2}\right) \right] - 1 \right) \tag{16}$$

In Eq. (45) are coefficients $a_1..a_7$ empirical data dependent on substance.

2. In the presented paper will be presented Chung-Lee-Starling model (CLS) [11-13]. Equations for the viscosity and the thermal conductivity are developed based on kinetic gas theories and correlated with the experimental data. The low-pressure transport properties are extended to fluids at high densities by introducing empirically correlated, density dependent functions. These correlations use acentric factor ω, dimesionless dipole moment μ_r and an empirically determined association parameters to characterize molecular structure effect of polyatomic molecules κ, the polar effect and the hydrogen bonding effect. In this paper are determined new constants for fluids.

The dilute gas viscosity for CLS model is written as:

$$\eta_0(T) = 26.69579 \cdot 10^{-1} \frac{\sqrt{MT}}{\Omega^{(2,2)*}\sigma^2} F_c \tag{17}$$

The factor F_c has been empirically found to be [12]:

$$F_c = 1 - 0.2756\omega + 0.059035\mu_r^{\ 4} + \kappa \tag{18}$$

where ω is the acentric factor, μ_r relative dipole moment and κ is a correction factor for hydrogen-bonding effect of associating substances such as alcohols, ethers, acitds and water.

For dense fluids Eq. (14) is extended to account for the effects of temperature and pressure by developing an empirically correlated function of density and temperature as shown below:

$$\eta = \eta_k + \eta_p \tag{19}$$

$$\eta_k = \eta_0\left(\frac{1}{G_2} + A_6 Y\right) \tag{20}$$

$$\eta_p = \left[36.344 \cdot 10^{-6} - (MT_c)^{.5} / V_C^{\ 2/3}\right] A_7 Y^2 G_2 x \exp(A_8 + A_9/T^* + A_{10}/T^{*2}) \tag{21}$$

$$Y = \rho V_c / 6, \quad G_1 = \frac{1.0 - 0.5Y}{(1.0 - Y)^3} \tag{22}$$

$$T_c = \frac{1.2593\varepsilon}{k}, \; V_c = \left(0.809\sigma(\text{Å})\right)^3 \tag{23}$$

$$G_2 = \frac{\{A_1(1 - \exp(-A_4 Y)) + A_2 G_1 \exp(A_5 Y) + A_3 G_1\}}{(A_1 A_4 + A_2 + A_3)} \tag{24}$$

The constants A_1-A_{10} are linear functions of acentric factor, reduced dipole moment and the association factor

$$A_i = a_0(i) + a_1(i)\omega + a_2(i)\mu_r{}^4 + a_3(i)\kappa, i=1,10 \quad (25)$$

where the coefficients a_0, a_1, a_2 and a_3 are presented in the work of Chung 2t al [11].

THE PREDICTION OF VISCOSITY OF GAS MIXTURES

For the determination of viscosity for dense gas mixtures we have used purely analytical model.[1,14] According to this theory the viscosity of dense gas mixtures containing N components can be written in the form:

$$\eta = -\frac{\begin{vmatrix} H_{11} & \cdots & H_{1N} & \psi_1 \\ \vdots & & \vdots & \vdots \\ H_{N1} & & H_{NN} & \psi_N \\ \psi_1 & & \psi_N & 0 \end{vmatrix}}{\begin{vmatrix} H_{11} & \cdots & H_{1N} \\ \vdots & & \vdots \\ H_{N1} & \cdots & H_{NN} \end{vmatrix}} \quad (26)$$

$$H_{ii} = \frac{\psi_i{}^2}{\eta_i} + \sum_{\substack{j=1 \\ j\neq i}}^{N} \frac{\psi_i \psi_j}{2\eta_{ij} A_{ij}^*} \frac{M_i M_j}{(M_i + M_j)^2} \left(\frac{20}{3} + \frac{4M_j}{M_i} A_{ij}^* \right) \quad (27)$$

$$H_{ij}(j \neq i) = -\frac{\psi_i \psi_j}{2\eta_{ij} A_{ij}^*} \frac{M_i M_j}{(M_i + M_j)^2} \left(\frac{20}{3} - 4A_{ij}^* \right) \quad (28)$$

where ρ is the molar density, ψ_i and ψ_j are mole fractions of species i and j, and M_i and M_j are their molecular masses. A_{ij}^* is a weak function of intermolecular potential for i-j interactions. The symbol η_i represents the viscosity of pure component i and η_{ij} represents the viscosity of i-j interaction.

RESULTS AND COMPARISON WITH EXPERIMENTAL DATA

Tables 1 and 2 show the difference in the speed of sound, for a mole fraction mxture of 70% methane and 30% carbon dioxide in the real gas region, calculated by models

based on isotropic statistical thermodynamics (JZG), non-isotropic models obtained from the perturbation part of the reference Lennard-Jones potential (JZG-LG) and models obtained by classical thermodynamics (BWR, BWRSN). In comparison with experimental results[42] somewhat larger deviations can however be found in the high-pressure region due to the large influence of the higher order multipolar, dispersion forces. On the basis of AAD (Table 1), we can conclude that the best results come from the JZG-LG model.

Due to spherical symmetry the molecules of methane have no dipole and quadrupole moments. The linear molecules of carbon dioxide, on the other hand, have a relatively very high effect of non-isotropic interactions resulting from the quadrupole moment.[2,3] Nevertheless, the results obtained by means of the JZG model show only about a 2% AAD (Table 1) due to a relatively small mole fraction of carbon dioxide. Table 2 shows ARVS in relation to pressure and temperature.

Analytical results are presented also as a function of the average absolute deviation – AAD and the absolute ratio of the speed of sound (ARVS)presented as:

$$ARVS = \mathrm{ABS}\left(\frac{c_{0non-isotropic} - c_{0\,isotropic}}{c_{0_{isotropic}}} \right), \tag{29}$$

where $c_{0isotropic}$ is the speed of sound obtained on the base of LJ (JZG) model. The greatest effect of non-isotropic interactions is found in the low temperature and high pressure region, where the contribution of non-isotropic interactions to the speed of sound is even higher than 4%.

Figures 1-3 show the deviation of the results for R32, R125 and mixtures R410A in the real gas region between the analytical computation (HH-Holland-Hanley model, CLS-Chung-Lee-Starling model and analytical results compared with REFPROP model

(version 23-7). The results for all models obtained by statistical thermodynamics show relatively good agreement. The computed viscosity conform well well for both models, obtained by statistical thermodynamics. The CLS model yield surprisingly good results.

CONCLUSION AND SUMMARY

The paper presents the mathematical model for computation of the velocity of sound in the fluid region.

For the real fluid, the Johnson-Zollweg-Gubbins model based on molecular dynamic and Lennard-Jones simulations and modified Benedict-Webb-Rubin equation of state (MBWR) was applied. In this paper are multipolar and induction interactions calculated with help of quantum mechanical calculation of the intermolecular energy function with help of Lucas-Gubbins perturbation theory. The multipole expansion is terminated at the octopole term.

The analytical results are compared with the experimental data obtained by dynamic light scattering technique, and they show a very good agreement.

The paper also presents the mathematical model for computation of viscosity in the liquid, and gaseus state.

The analytical results are compared with the dynamic light scattering and show relatively good agreement. In the region of real gases the results are an equally good match.

LITERATURE

13. K. Lucas, *Applied Statistical Thermodynamics* (Springer-Verlag, New York, 1992).

2. B.J. McClelland, *Statistical Thermodynamics* (*Chapman & Hall, London, 1980).*

3. C.G. Gray, K.E. Gubbins*, Theory of Molecular Fluids* (Clarendon Press, Oxford, 1984).

4. B.J. Moser, *Die Theorie der Intermolekularen Wechseelwirkungen und Ihre Anwendung auf die Berechnung von Verdampfungsgleichgewichten binärer Systeme*", PhD Thsesis (Universität Duisburg, Germany, 1981).

5. L.K. Johnson, J.A. Zollweg, K.E. Gubbins, Molecular Physics, **78**:591 (1993).

6. J.H. Ferziger, H.G. Kasper, *Mathematical Theory of Transport Processes in Gasses* (North-Holland Publishing Company, London, 1972)

7. P.D. Neufeld, A.R. Janzen, R.A. Aziz, The Journal of Chemical Physics, **57**:1100.

8. F. R.W. McCourt, J.J. Beenakker, W.E. Köhler, I. Kuscer, I., *Nonequilibrium Phenomena in Polyatomic gases* (Clarendon Press, London, 1990).

9. S.B. Kiselev, R.A. Perkins, M.L. Huber, International Journal of Refrigeration, **22**:509 (1999).

10. S.B. Kiselev, M.L. Huber, Fluid Phase Equilibria,**142**:253(1998).

11. T.-H. Chung, L.L. Lee, K.E. Starling, Ind. Eng. Chem. Res., **27**:671 (1988).

12. T.-H. Chung, M. Ajlan, L.L. Lee, K.E. Starling, Ind. Eng. Chem. Fundam., **23**:8 (1984).

13. W.H. Xiang, Fluid Phase Equilibria, **187-188**:221 (2001).

14. V.Vesovic, W. Wakeham, International Journal of Thermophysics, **10**:125 (1989).

Table 1. Comparison between analytical results and experimental speed of sound data for mixture of 70% R 50 and 30% R 744.

Temp.	Model	10 bar	20 bar	60 bar	100 bar	AAD* (%)
			c_0 (m/s)			
250 K	JZG	329	323	301.6	300	0.022364
	BWR	332.4	315.2	277.5	272.1	0.047959
	BWRSN	332.3	314.9	282.9	323.7	0.021633
	JZG-LG	329.8	323	288.8	313.1	0.006061
	Exp.[42]	329	319	290	311.5	

*AAD= average absolute deviation

Table 2. Influence of absolute ratio speed of sound (ARVS) for a mixture of 70% R 50 and 30% R 744 (JZG-LG model).

	ARVS			
	10 bar	20 bar	60 bar	100 bar
250 K	0.002432	0.000929	0.04244	0.043667
300 K	0	0.000279	0.001141	0.000859
350 K	0	0	0.00026	0.000517

FIGURE CAPTIONS:

Fig 1: Kinematic viscosity of R32 in the region of saturated vapour

Fig 2: Kinematic viscosity of R125 in the region of saturated vapour

Fig 3: Kinematic viscosity of R410A in the region of saturated vapour

FIGURES

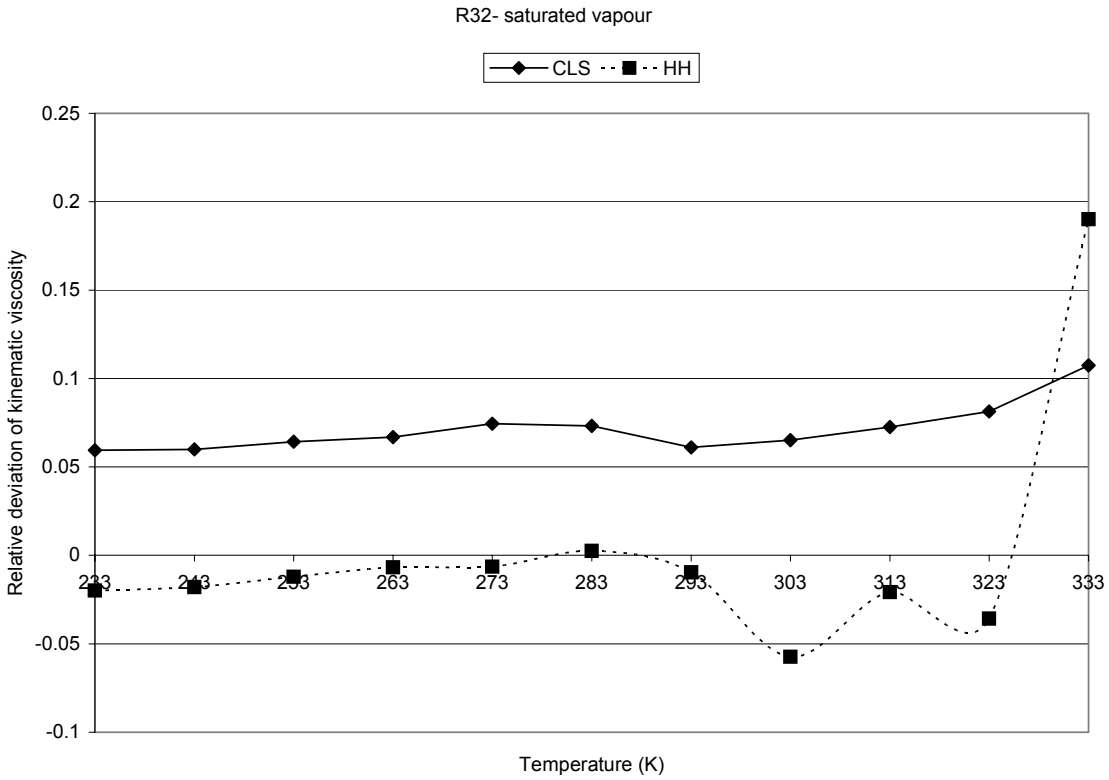

Fig 1: Kinematic viscosity of R32 in the region of saturated vapour

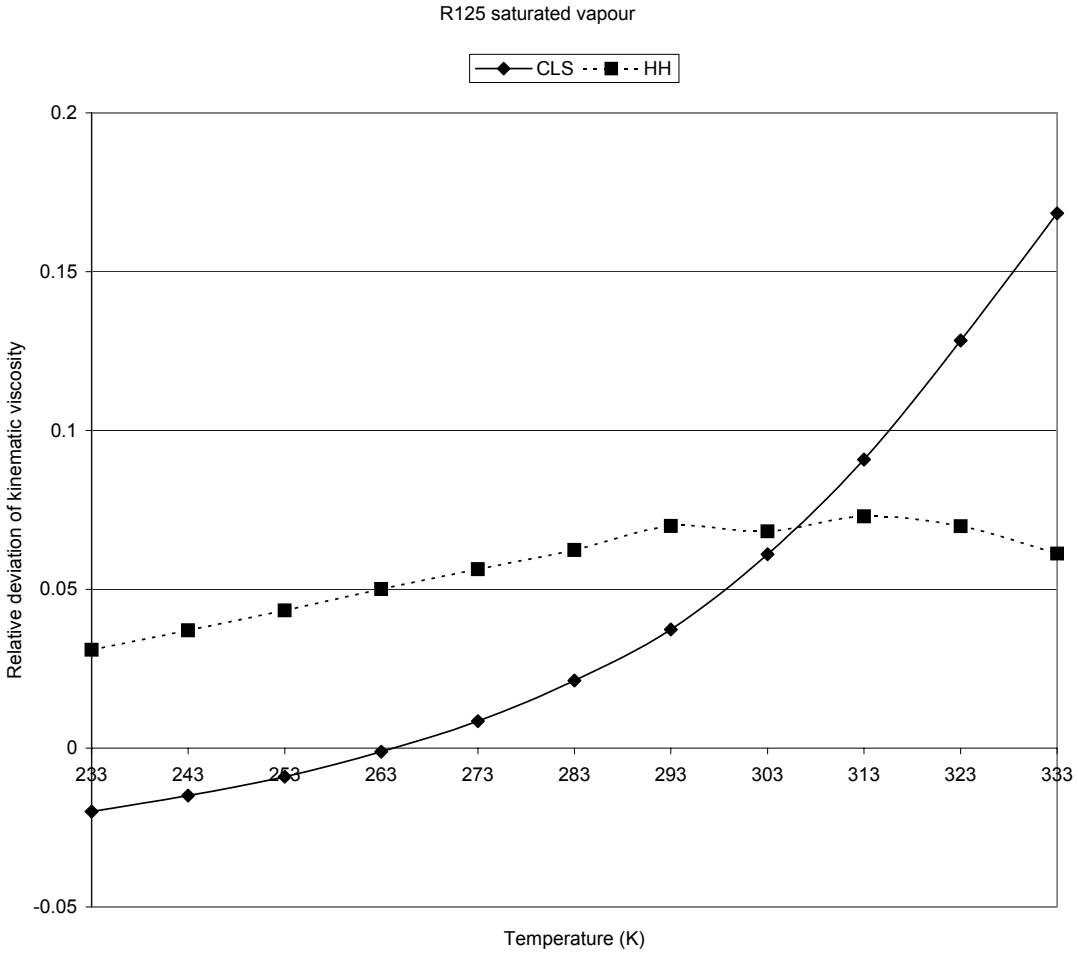

Fig 2: Kinematic viscosity of R125 in the region of saturated vapour

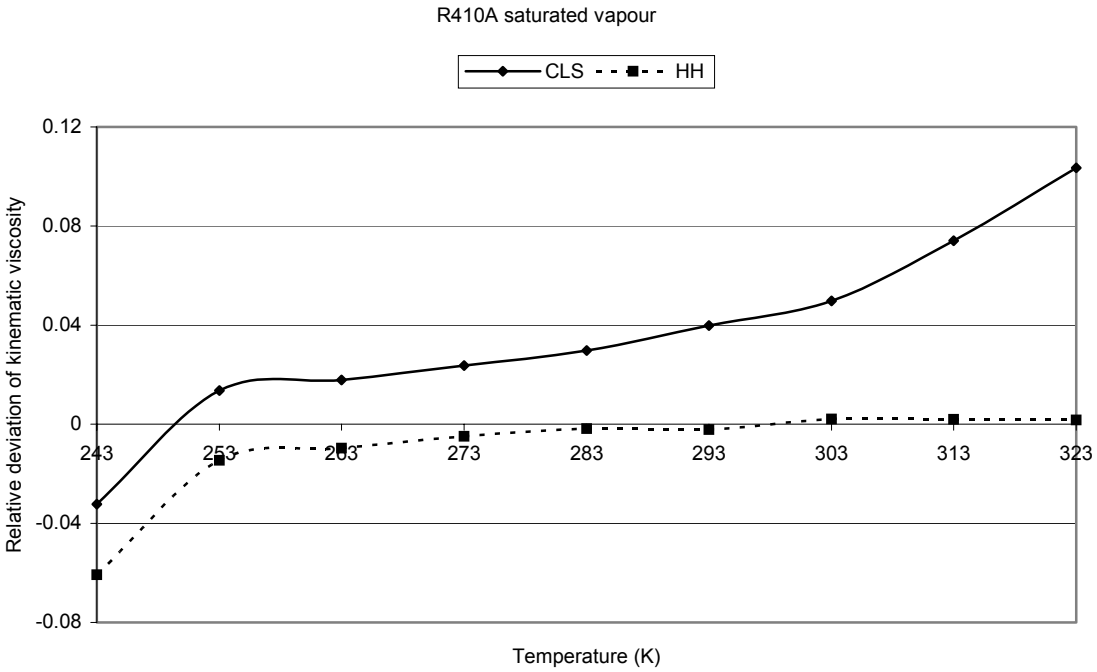

Fig 3: Kinematic viscosity of R410A in the region of saturated vapour